RSC Advances

ROYAL SOCIETY OF CHEMISTRY

www.rsc.org/advances

Table of Contents

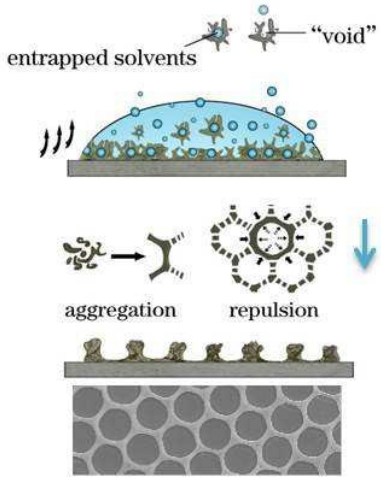

The schematic diagram of honeycomb structure formation from AOB-t8.

Journal Name

ARTICLE

Single-Step Fabrication of Large-Scale Patterned Honeycomb Structures via Self-Assembly of a Small Organic Molecule

Received 00th January 20xx,
Accepted 00th January 20xx

DOI: 10.1039/x0xx00000x

www.rsc.org/

Xia Ran,[a] Kun Zhang,[a] Lili Shi,[a] Zhen Chi,[a] Weihong Qiu[b,*] and Lijun Guo[a,*]

Microstructures with regular patterns, in particular, honeycomb-patterned structures have attracted extensive attention in various applications, such as photonic crystals, cell cultures, protein patterning, superhydrophobic coatings. Here we report the successful single-step fabrication of large-scale honeycomb-patterned structures on a variety of substrates via self-assembly of an azobenzene derivative, N-(3,4,5-octanoxyphenyl)-N'-4-[(4-hydroxyphenyl)azophenyl] 1,3,4-oxadiazole (AOB-t8). Factors such as concentration, substrate, solvent evaporation temperature and the relative humidity are revealed to be able to control the size of the formed micropores. A model to describe the dynamical formation of honeycomb structures from AOB-t8 has been proposed. The used method in this work demonstrates the potential to open up new possibilities for preparing large-scale, orderly structured materials from low mass organic molecules, which is of significance in a variety of potential applications.

Introduction

Microstructures with regular patterns are of great interest because of their ordered morphologies, controllable sizes, and excellent biocompatibility.[1] In particular, two- and three-dimensional honeycomb-patterned films at micrometer scale have been used in photonic crystals,[2] scaffolds for biological cells or proteins,[3] templates for nanomaterials,[4] superhydrophobic coatings,[5] surface-enhanced Raman spectroscopy,[6] and dye-sensitized solar cells.[7] The preparation of ordered macroporous structures usually requires prefabricated templates involving multiple steps, which increases the complexity of fabrication process and may result in damage to the final structures. Recently, the breath figure (BF) method is an effective dynamic template approach for fabricating ordered honeycomb structures from a variety of different materials, including linear polymers, star-like polymers, block copolymers, dendronized polymers, amphiphilic copolymer, and organic-inorganic hybrid complexes.[8] The reported works mainly used the neat polymer molecules or the assisted polymer molecules. Despite the fact that small organic molecules have well-defined molecular structures and are easy synthesize and modify, they are rarely used to fabricate the honeycomb structures via the BF methodology,[9,10] because most small organic molecules have the propensity to crystallize during the solvent evaporation process.

In this work, we report the fabrication of large-scale honeycomb-patterned structures with controllable pore sizes on a variety of substrates by the self-assembly of N-(3,4,5-octanoxyphenyl)-N'-4-[(4-hydroxyphenyl)azophenyl] 1,3,4-oxadiazole (AOB-t8). The synthesis of AOB-t8 was reported in our previous work.[11] As illustrated in Scheme 1, AOB-t8 is a rod-coil oxadiazole derivative consisting of hydroxyl, azobenzene and 1,3,4-oxadiazole moieties with three alkyl chains. To choose AOB-t8 as the organogelator for the current work is on the basis of that the molecule has the potential to form hydrogen bonds via the hydroxyl groups, π-π interaction via the azobenzene and 1,3,4-oxadiazole moieties, and Van der Waals force via the three alkyl chains, all of which would collectively drive the small organic molecule to self-associate. The important feature of this work is adopting supramolecular self-assembly of a small organic molecule containing multiple intermolecular interactions to prepare a large-scale, highly ordered hexagonal pattern with a one-step, simple and practicable approach. Moreover, an alternative mechanism is proposed to illustrate how the morphology dynamically transforms from sol to various substrates.

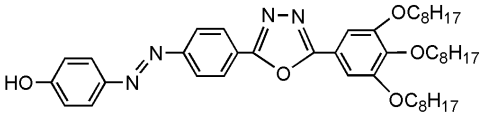

AOB-t8

Scheme 1 Molecular structure of AOB-t8.

Experimental

Field emission scanning electron microscopy (FE-SEM) images were taken with a JSM-6700F apparatus. For the observation of honeycomb-patterned structures, a small drop of AOB-t8 in DCE was casted on several common substrates and allowed to undergo

[a] Department of Physics, School of Physics and Electronics, Henan University, Kaifeng 475004, People's Republic of China. E-mail: juneguo@henu.edu.cn
[b] Department of Physics, Oregon State University, Corvallis OR 97331, USA. Email: Weihong.Qiu@physics.oregonstate.edu.
† Electronic Supplementary Information (ESI) available. See
DOI: 10.1039/x0xx000000

rapid solvent evaporation for forming patterned microporous structures at different temperature. The sample was pressed into a tablet with KBr for FT-IR measurement. FT-IR spectra were recorded with a Perkin-Elmer spectrometer (Spectrum One B). UV-vis absorption spectra were recorded on a Shimadzu UV-2550 spectrometer. A representative optical micrograph were recorded on optical microscope with Evolve 512 Delta EMCCD (photometrics) camera using oil immersion TIRF lens (1.45NA, 100×, Nikon), incorporating a wide-field light source.

Results and discussion

The noncovalent interactions, such as hydrogen bonding, π-π stacking and Van der Waals interaction, play a mutual balance to modulate the packing arrangement of molecules and eventually construct a particular superstructure and functional surface. The numerous interactions in AOB-t8 should offer, at least to some extent, the possibility in controlling the aggregation morphology. We firstly attempted to prepare the ordered honeycomb structures on a silicon substrate from 1×10^{-3} M AOB-t8. Briefly, a small drop of AOB-t8 in dichloromethane (DCE) was casted on silicon plate and allowed to undergo rapid solvent evaporation for forming patterned microporous structure (as shown in Figure 1(c)). To find the optimum conditions for the formation of the ordered honeycomb microstructure, SEM images of AOB-t8 in dichloromethane with different concentrations ranging from 1×10^{-5} M to 1×10^{-2} M at 20°C and 60% relative humidity (R. H.) were obtained. Figure 1 shows the scanning electron microscopy (SEM) images of the resulting drop-cast films, which shows that hexagonal honeycomb structures can be readily obtained for a broad range of AOB-t8 concentrations albeit with different pore sizes. The only exception is 1×10^{-5} M AOB-t8 in DCE, as the SEM image features an irregular meshwork with circular structures of ~500 nm in diameter and wire-like fibers with the width of ~20-50 nm (Fig. 1(a)). At 1×10^{-4} M AOB-t8 in DCE, it can be observed that the average pore size of ordered hexagonal honeycomb structures is of ~5.0 μm in a large area. The honeycomb structure becomes more regular as the concentration of AOB-t8 increases to 1×10^{-3} M, featuring a large area of hexagonal porous structure with an average pore size of ~2.5 μm in diameter (Fig. 1(c)). At 1×10^{-2} M AOB-t8 in DCE, the pore size is ~1.5 μm in diameter on average, and layers of honeycomb structures appear to stack on top of each other, suggesting that the honeycomb structures likely grow in a layer-by-layer mode.

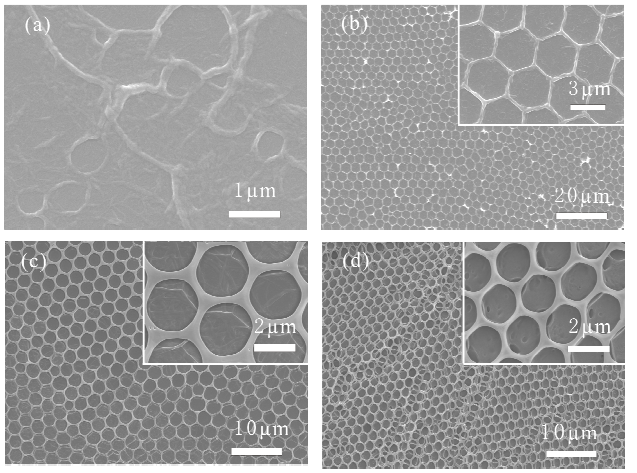

Figure 1 SEM images of the drop-cast films derived from AOB-t8 at different concentrations in DCE: (a) 1×10^{-5} M, (b) 1×10^{-4}, (c) 1×10^{-3} M and (d) 1×10^{-2} M on silicon at 20°C and 60% relative humidity (R. H.).

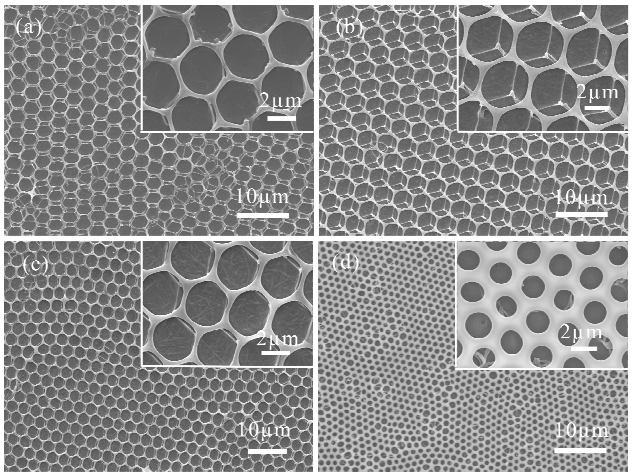

Figure 2 SEM images of the honeycomb-patterned structures derived from AOB-t8 (1×10^{-3} M) in DCE at 20°C and 60% R. H. on (a) quartz (b) glass (c) graphite and (d) PVC sheet.

To extend the potential application of ordered honeycomb structure, we selected several frequently-used substrates and employed our one-step method to prepare and investigate the morphology of self-assembly structures from AOB-t8 (1×10^{-3}M) in dichloromethane. Surprisingly, the honeycomb structure can be obtained on a variety of substrates, such as quartz, glass, graphite and so on. The SEM images (Figure 2) on different substrates indicate AOB-t8 a versatile feature in constructing ordered honeycomb structure, even though slightly different characteristics could be observed to some extent. These inorganic and solid substrates represent the more classical supports on which honeycomb-like structures have been elaborated. The observations for AOB-t8 indicate that the hexagonal honeycomb array on quartz, glass and graphite substrates can be formed over a very large area without theoretical scale limit in two dimension structure, which was confirmed from the optical micrograph (Figure S1) of the film on glass plate at room temperature. The average pore diameter of honeycomb on glass substrate is around 5.8 μm with the wall thickness of around 461 nm, which is larger than that on other substrates. Meanwhile, the upper and lower honeycomb structured layers demonstrates an obvious dislocation, supporting the mentioned above growth mode from bottom to top. Therefore, the pore size of honeycomb

unit can be simply tuned by altering the concentration of AOB-t8 solution as well as the substrates, which is of significance for the potential applications. Compared with previous demanding conditions, the method used in this work is more effective and maneuverable in practical areas. So far, an important challenge is to reproduce this highly organized structure on a soft and flexible organic surface. For instance, PVC sheet has been chosen as a current, transparent and flexible polymeric material. The obtained SEM images after casting the solution of AOB-t8 in dichloromethane on a PVC sheet are shown in Fig. 2d. Unexpectedly, a similar honeycomb structure in a hexagonal array over a large scale is also observed on this organic surface. The average size of hexagonal unit is around 1.9 μm in diameter, two times smaller than that on glass surface.

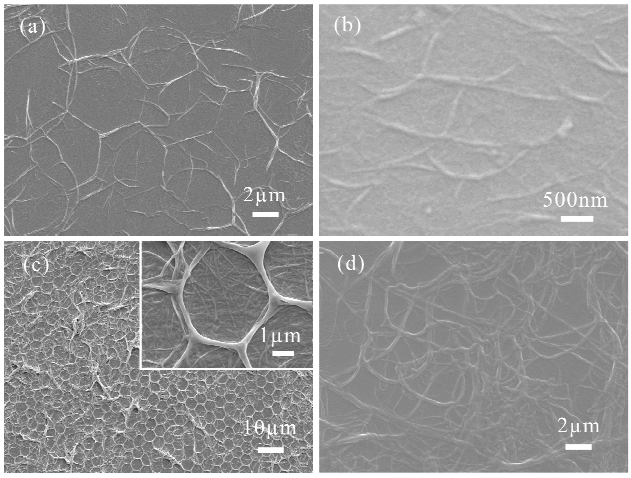

Figure 3 SEM images of the macroporous structures derived from AOB-t8 at different concentrations in DCE and at different temperatures: (a) 1×10^{-4} M at 5°C, (b) 1×10^{-4} M at 50°C, (c) 1×10^{-3} M at 5°C and (d) 1×10^{-3} M at 50°C on silicon plates. The relative humidity was kept at 60% for all four experiments.

As is known, the temperature control during the casting process can affect the evaporation, condensation, surface tension, viscosity of the solution and solubility. By adjusting the initial temperature of substrates, it is found the temperature imposes an important effect on the formation of ordered pattern. In contrast to the highly ordered honeycomb structure formed at 20°C and 60% relative humidity (R. H.) (Fig. 1), the SEM images from the solution of AOB-t8 at other two different temperature (5°C and 50°C) are shown in Figure 3. For 1×10^{-4} M AOB-t8 in DCE, the SEM images of the drop-cast films features fragmentary hexagonal arrays and disordered fibers at 5°C (Fig. 3(a)) and entangled and dense fibrous aggregates at 50 °C (Fig. 3(b)), both in sharp contrast to the highly regular honeycomb-patterned structures at 20°C with the same AOB-t8 concentration and relative humidity (Fig. 1(b)). Similarly, for 1×10^{-3} M AOB-t8 in DCE at 60% relative humidity, the SEM images of the macroporous structures are much less regular at both 5°C and 50°C (Fig. 3(c) and 3(d)) than that at 20°C (Fig.1(c)), which features a highly regular honeycomb-patterned structures. These observations confirm that temperature is a critical determinant for forming the honeycomb-patterned structures via the self-assembly of AOB-t8.

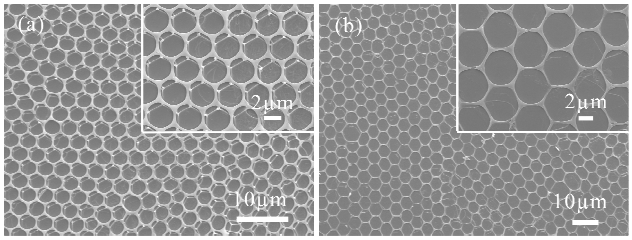

Figure 4 SEM images of the honeycomb-patterned structures from 1×10^{-3} M AOB-t8 in DCE with the relative humidity of: (a) 20% and (b) 80% on silicon substrates. The temperature was kept at 20°C.

Relative humidity is a key parameter in the BF technique, and a relative humidity of 50% or higher is typically required for forming honeycomb-patterned structures.[8] In the current work, we performed all the castings in a customized perspex glove box, which allowed us to vary the humidity levels while keeping other parameters constant. Figure 4 shows the honeycomb-patterned structures derived from 1×10^{-3} M AOB-t8 in DCE at 20°C and two different relative humidity levels: 20% and 80%. At 20% R. H., it was observed a hexagonal honeycomb array with highly homogeneous pores of ~3 μm in diameter (Fig. 4(a)), similar to that derived at 60% R. H. with the same AOB-t8 concentration and environment temperature (Fig. 1(c)). When the relative humidity was set at 80% R. H., the honeycomb porous arrangement was still able to be observed, which contains inhomogeneous hexagonal arrays and pores of much larger diameters. These results suggest that honeycomb-patterned structures can be obtained via the self-assembly of AOB-t8 at a wide range of relative humidity levels, and the environment relative humidity is not as critical for AOB-t8 as for other gelators.

Azobenzene and its derivatives are well known for their photochromic properties because they can undergo *trans*–*cis* isomerization. When the honeycomb-patterned film formed by AOB-t8 was irradiated with 365 nm light from a 250 W high-pressure mercury lamp, the UV-vis spectra of the film (Figure S2) showed that the π–π* absorption of *trans*-azobenzene moiety decreased with the irradiation time, indicating a photoinduced *trans*-to-*cis* isomerization. It was found that the conversion to *cis*- from *trans*- azobenzene can reach ca. 20% in the photostationary state after 5 hours UV irradiation, demonstrating that it is difficult to photoinduce the *trans*-to-*cis* isomerization for AOB-t8 films compared with AOB-t8 in solution.[12, 13] Consistently, the scanning electron microscopy images suggest that the large-scale, highly ordered hexagonal pattern become irregular after UV irradiation for 5 hours at room temperature, as shown in Figure S3.

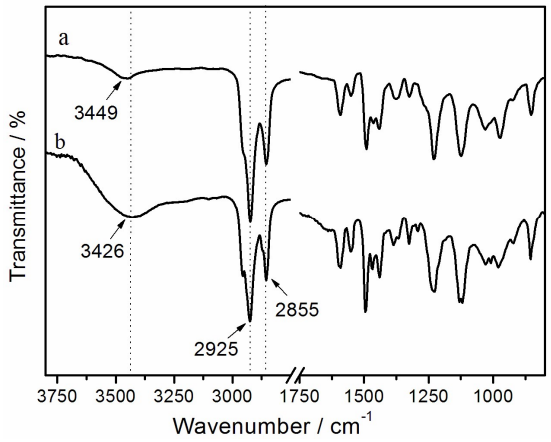

Figure 5 FT-IR spectra of (a) the macro-porous film formed by 1×10^{-3} M AOB-t8 in DCE and (b) AOB-t8 powder from DCE.

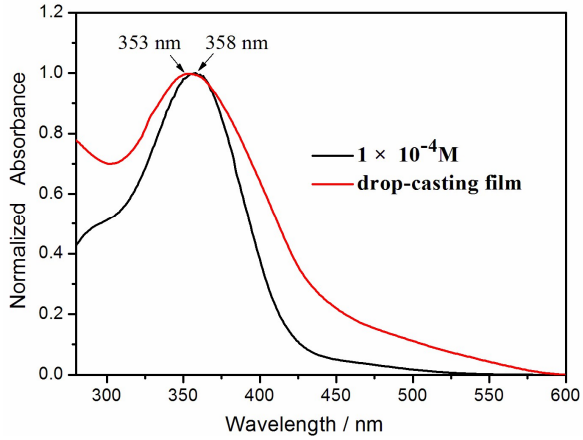

Figure 6 Normalized UV-Vis absorption spectra of 1×10^{-4} M AOB-t8 in DCE and AOB-t8 in the drop-casting film.

To determine the molecular interactions and alkyl chain conformations underlying the self-assembly process of these honeycomb films, the FT-IR and absorption spectra of AOB-t8 were measured. For drop-cast films formed by 1×10^{-3} M AOB-t8 in DCE, the vibration mode of hydrogen-bonded O-H stretching is at 3449 cm^{-1}, while the peak is slightly shifted to the lower wavenumber of 3426 cm^{-1} for the AOB-t8 powder (Figure 5). This shift suggests that the hydrogen bonds in the drop-cast films are more disordered than those in the AOB-t8 powder.[14] On the other hand, the $\nu_s(CH_2)$ and $\nu_{as}(CH_2)$ are at ~2855 and 2925 cm^{-1}, respectively, for both drop-cast films and the AOB-t8 powder, implying that the alkyl chains are tightly packed to form quasi-crystalline domains.[15] The absorption maximum is at 358 nm for 1×10^{-4} M AOB-t8 in DCE (Figure 6), and is slightly blue-shifted to 353 nm in the drop-cast films, indicating that the azobenzene units form H-type aggregates through π-π interactions.[16]

Surface roughness is an important factor to affect the surface hydrophobicity according to the Wenzel's equation.[17] The wettability of film can be characterized by measuring the water contact angle on the surface. The shapes of a water droplet sitting on the honeycomb-patterned film from 1×10^{-3} M AOB-t8 in DCE on glass and PV sheet are shown in Figure S4. The static contact angle of water on the honeycomb-patterned film on glass with a pore size of around 5.8 μm is ca. 125°, which is larger than that (ca. 108°) on the film of smaller pores (around 1.9 μm in diameter) prepared on PV sheet. The results indicate that the increase of the film roughness enhances the surface hydrophobicity of honeycomb structure, implying that the surface wettability can be feasibly controlled by changing experimental conditions for film formation.

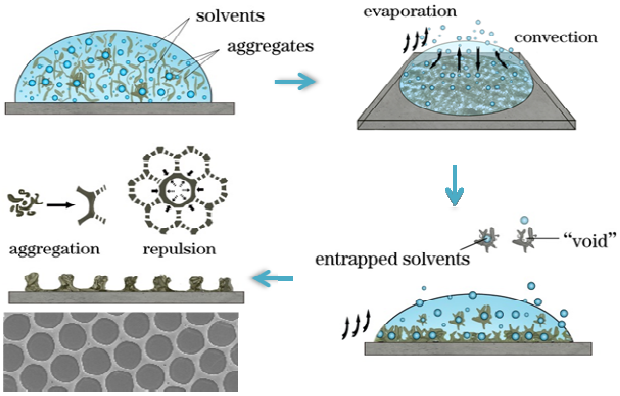

Figure 7 The schematic diagram of honeycomb structure formation process from AOB-t8 gelator.

Recently, Kim and co-workers used a small molecule to obtain a hierarchical honeycomb structure via the BF method, whereby water droplets were formed during the process of solvent evaporation that resulted in the self-organization of aggregates around the droplets.[9a] Yi and co-workers proposed a vesicle mechanism for the formation of macroporous structures, in which the rupture of vesicles and the molecular motion collectively drive the formation of hexagonal grid-like patterns.[10] In our experiments with the organogelator AOB-t8, the formation of honeycomb-patterned structures is independent on the relative humidity levels and the ordered honeycomb structures can be formed in a broad range of R.H. levels from 20% to 80%. Meanwhile, there is no vesicle observed in our experiments. Thus, neither of the aforementioned models is applicable to the honeycomb structure derived from AOB-t8 in this work, and the process of honeycomb structure formation from AOB-t8 could be illustrated in a schematic diagram (Figure 7). It was previously demonstrated that the small organic gelator AOB-t8 has the propensity to self-associate to form aggregates such as particles, strands, fibers and even network-like structures, and the self-assembly is largely driven by hydrogen-bonding, π-π interactions and van der Walls interactions mediated by the gelling solvents.[11] In the AOB-t8 DCE organogel, the DCE

solvent molecules are entrapped within the AOB-t8 aggregates. When the organogel is casted as droplets onto the surface of a substrate, these AOB-t8 aggregates (strands, fibers, etc.) instantly adhere to the substrate surface, as evidenced by those irregular macroporous structures underneath the ordered honeycomb structures for all substrates (Fig. 1). The entrapped solvent molecules then move upward during the solvent evaporation process, leaving "voids" all over the substrate surface. The "voids" continue to grow because of the propensity of AOB-t8 to self-assemble. Subsequently, free AOB-t8 molecules, particles, strands and fibers rearrange around these "voids" to form the precursor honeycomb structures precursor of honeycomb structures, likely in a manner similar to the vesicles model by Yi and co-workers.[10] Simultaneously, the solvent evaporation process cools down the top surface of the droplets to generate a temperature gradient between the top and bottom of the droplet, and the surface tension is enhanced by the upward flow of warmer liquid. As a consequence, the self-assembly of AOB-t8 around the "voids" creates an effective "attraction force" outward the pore, while an effective inward "repulsive force" is developed between adjacent units. The balance between the "attractive" and "repulsive" forces, mediated by surface tension, dissipation and the frictional effect of viscosity, drives the formation of highly ordered honeycomb patterns with a hexagonal pore for AOB-t8 in DCE. It should be pointed out that the rod-coil shape of the organogelator AOB-t8 likely also plays an important role during the formation of such ordered structures.[10] However, it still remains to be determined the entire dynamical process for the formation of highly ordered honeycomb structures from a small organic molecule such as AOB-t8.

Conclusions

In summary, large-scale highly ordered honeycomb structures have been successfully fabricated by the self-assembly of AOB-t8. Patterned honeycomb structures can be readily obtained by casting the DCE solution containing AOB-t8 on both inorganic and flexible organic substrates. An alternative model has been proposed to describe the dynamical formation of honeycomb structures from AOB-t8. The method used in this work demonstrates the potential to open up new possibilities for preparing large-scale, orderly structured materials from low mass organic molecules, which is of great importance in a variety of potential applications.

Acknowledgements

The authors are grateful to the National Science Foundation Committee of China (project No. 21173068) and the Program for Innovative Research Team in University of Henan Province (No. 13IRTSTHN017) for their financial support of this work.

Notes and references

1 (a) J. L. Atwood, J. W. Steed, Organic Nanostructures, Wiley-VCH, Weinheim, Germany, 2008; (b) H. Ma, J. Hao, *Chem. Soc. Rev.,* 2011, **40**, 5457; (c) J. Ma, Y. S. Hui, M. Zhang, Y. Yu, W. Wen, J. Qin, *small*, 2013, **9**, 497; (d) L. C. Palmer and S. I. Stupp, *Acc. Chem. Res.*, 2008, **41**, 1674; (e) X. Dou, W. Pisula, J. Wu, G. J. Bodwell and K. Mullen, *Chem.-Eur. J.*, 2008, **14**, 240; (f) A. Ajayaghosh and V. K. Praveen, *Acc. Chem. Res.*, 2007, **40**, 644; (g) M. Suzuki and K. Hanabusa, Chem. Soc. Rev., 2009, 38,967; (h) S. Kiyonaka, K. Sada, I. Yoshimura, S. Shinkai, N. Kato, I. Hamachi, *Nat. Mater.,* 2004, **3**, 58.

2 S. Kubo, Z. Z. Gu, K. Takahashi, A. Fujishima, H. Segawa, O. Sato, *J. Am. Chem. Soc.,* 2004, **126**, 8314.

3 (a) T. Nishikawa, M. Nonomura, K. Arai, J. Hayashi, T. Sawadaishi, Y. Nishiura, M. Hara, M. Shimomura, *Langmuir*, 2003, **19**, 6193; (b) D. Beattie, K. H. Wong, C. Williams, L. A. Poole-Warren, T. P. Davis, C. Barner-Kowollik, M. H. Stenzel, *Biomacromolecules*, 2006, **7**, 1072; (c) M. Hernandez-Guerrero; E. Min, C. Barner-Kowollik, A. H. E. Muller, M. H. Stenzel, *J. Mater. Chem.,* 2008, **18**, 4718; (d) E. Min, K. H. Wong, M. H. Stenzel, *Adv. Mater.*, 2008, **20**, 3550; (e) L. Li, C. Chen, J. Li, A. Zhang, X. Liu, B. Xu, S. Gao, G. Jin, Z. Ma, *J. Mater. Chem.*, 2009, **19**, 2789.

4 (a) A. Boker, Y. Lin, K. Chiapperini, R. Horowitz, M. Thompson, V. Carreon, T. Xu, C. Abetz, H. Skaff, A. D. Dinsmore, T. Emrick, T. P. Russell, *Nature Mater.,* 2004, **3**, 302; (b) W. Sun, J. Ji, J. C. Shen, *Langmuir*, 2008, **24**, 11338; (c) M. H. Nurmawati, P. K. Ajikumar, R. Renu, S. Valiyaveettil, *Adv. Funct. Mater.*, 2008, **18**, 3213; (d) C. Li, G. S. Hong, P. W. Wang, D. P. Yu, L. M. Qi, *Chem. Mater.,* 2009, **21**, 891.

5 (a) Y. Gao, Y. Huang, S. Xu, W. Ouyang, Y. Jiang, *Langmuir*, **2011**, 27, 2958; (b) H. Yabu, Y. Hirai, M. Kojima, M. Shimomura, *Chem. Mater.,* 2009, **21**, 1787.

6 M. Guerrero, M. H. Stenzel, *Polym. Chem.*, 2012, **3**, 563.

7 E. S. Kwak, W. Lee, N. G. Park, J. Kim, H. Lee, *Adv. Funct. Mater.,* 2009, **19**, 1093.

8 (a) J. Kim, E. Lee, Y. Jeong, J. Lee, W. Zin, M. Lee, *J. Am. Chem. Soc.,* 2007, **129**, 6082; (b) L. A. Connal, P. A. Gurr, G. G. Qiao, D. H. Solomon, *J. Mater. Chem.,* 2005, **15**, 1286; (c) C. Deleuze, C. Derail, M. H. Delvilleb, L. Billon, *Soft Matter*, 2012, **8**, 8559; (d) K. H. Wong, M. H. Stenzel, S. Duvall, F. Ladouceur, *Chem. Mater.,* 2010, **22**, 1878; (e) L. Li,; Y. Zhong,; J. Gong,; J. Li, C. Chen, B. Zenga, Z. Ma, *Soft Matter*, 2011, **7**, 546; (f) H. Ma, J. Cui, A. Song, J. Hao, *Chem. Commun.,* 2011, **47**, 1154. (g) M. H. Guerrero, M. H. Stenzel, *Polym. Chem.*, 2012, **3**, 563. (h) Liu, C. H.; Gao, C.; Yan, D. Y. *Angew. Chem., Int. Ed.,* 2007, **46**, 4128; (i) K. H. Wong, M. H. Stenzel, S. Duvall, F. Ladouceur, *Chem. Mater.,* 2010, **22**, 1878.

9 (a) J. H. Kim, M. Seo, S. Y. Kim, *Adv. Mater.,* 2009, **21**, 4130; (b) Y. Yu, Y. Ma, Soft Matter, 2011, 7, 884; (c) M. Lee, B.-K.Cho, K. J. Ihn, W.-K. Lee, N-K Oh, W-C Zin, J. Am. Chem. Soc. 2001, 123, 4647; (d) Y.-F. Gao, Y.-J. Huang, S.-Y. Xu, W.-J. Ouyang, Y.-B. Jiang, *Langmuir*, 2011, **27**, 2958; (e) L. Heng, W. Qin, S. Chen, R. Hu, J. Li, N. Zhao, S. Wang, B. Z. Tang, L. Jiang, *J. Mater. Chem.,* 2012, **22**, 15869. (f) S. S. Babu, S. Mahesh, K. K. Kartha and A. Ajayaghosh, *Chem.-Asian J.*, 2009, **4**, 824.

10 M. Zhang, S. Sun, X. Yu, X. Cao, Y. Zou, T. Yi, *Chem. Commun.*, 2010, **46**, 3553.

11 X. Ran, H. Wang, J. Lou, L. Shi, B. Liu, M. Li, L. Guo, *Soft Materials*, 2014, **12**, 396.

12 M. Han and K. Ichimura, *Macromolecules*, 2001, **34**, 82.

13 X. Ran, H. Wang, L. Shi, J. Lou, B. Liu, M. Li and L. Guo, *J. Mater. Chem. C*, 2014, **2**, 9866.

14 C. Xue, S. Jin, X. Weng, J. J. Ge, Z. Shen, H. Shen, M. J. Graham, J. K. Jeong, H. Huang, D. Zhang, M. Guo, F. W. Harris, S. Z. D. Cheng, *Chem. Mater.*, 2004, **16**, 1014.

15 N. V. Venkataraman, S. Vasudevan, *J. Phys. Chem. B*, 2001, **105**, 1805.

16 (a)H. Kobayashi, K. Koumoto, J. H. Jung, S. Shinkai, *J. Chem. Soc., Perkin Trans.,* 2002, **2**, 1930;(b) X. Ran, H. Wang, L. Shi, J. Lou, B. Liu, M. Li, L. Guo, *J. Mater. Chem. C,* 2014, **2**, 9866.
17 R. N.Wenzel, *Ind. Eng. Chem.*, 1936, **28**, 988.